Liu, X., Kamliya Jawahar, H., Azarpeyvand, M., & Theunissen, R. (2015). Aerodynamic and Aeroacoustic Performance of Serrated Airfoils. In 21st AIAA/CEAS Aeroacoustics Conference. [AIAA 2015-2201] American Institute of Aeronautics and Astronautics Inc, AIAA. DOI: 10.2514/6.2015-2201

Aerodynamic and Aeroacoustic Performance of Serrated Airfoils

X. Liu[1], H. Kamliya Jawahar[1], M. Azarpeyvand[2] and R. Theunissen[3]
University of Bristol, Bristol, United Kindom, BS8 1TR

The aerodynamic and aeroacoustic performance of serrated airfoils have been studied experimentally. A comprehensive aerodynamic study of a symmetric (NACA 0012) and an asymmetric (NACA 65(12)-10) airfoil with different types of trailing-edge serrations has been performed. Steady aerodynamic force measurements over a wide range of Reynolds number and angles of attack has been carried out. Results have shown that the use of trailing-edge serrations can generally lead to a significant reduction in the airfoil lift coefficient. It has also been shown that the most effective serrations, in terms of noise reduction, namely the sharp sawtooth and slotted-sawtooth, cause the highest level of lift reduction. Two-dimensional Laser Doppler Anemometry (LDA) and hotwire tests have also been carried out in order to better understand the effects of trailing-edge serrations on wake development. Results have also shown that the use of trailing-edge serrations leads to significant reduction in the airfoil's wake turbulence level, which appears to have been caused due to the interaction between flow field over the tip and root planes. Preliminary experimental results confirm that passive flow control methods, such as serrations, used for airfoil noise reduction can significantly affect the aerodynamic performance of the airfoil.

Nomenclature

Re_c	=	chord based Reynolds number
$2h$	=	amplitude of serration
α	=	angle of attack
C	=	chord length
α_s	=	serration angle
λ	=	serration wavelength
d	=	slot width
H	=	slot depth
U	=	wind speed
U_0	=	freestream wind speed
AoA	=	Angle of Attack
C_L	=	lift coefficient
$C_{L,max}$	=	maximum lift coefficient
C_D	=	drag coefficient
TKE	=	turbulence kinetic energy
$\overline{u'u'}$	=	Streamwise Reynold normal stress
$\overline{v'v'}$	=	Spanwise Reynold normal stress
$\overline{u'v'}$	=	Reynolds shear stress

[1] Department of Mechanical Engineering, University of Bristol, PhD student.
[2] Department of Mechanical Engineering, University of Bristol, Lecturer and Royal Academy of Engineering research fellow.
[3] Department of Aerospace Engineering, University of Bristol, Lecturer.

I. Introduction

Aviation has an indisputable role in modern society in the 21st century. Air travel in Europe has risen three-fold over the past two decades since 1980 and is set to double by 2020. The increasing popularity of air travel and rapidly increasing airports has lead to stringent standards being set by ICAO for aircraft noise control. This has made aero-acoustics a major area of interest. A number of aerodynamic noise sources, such as engines, landing gears, airframes and fuselage generates aircraft noise. The engine noise has been considerably reduced over the past few decades due to increase in bypass ratio along with the proper design and application of the engine nacelle. However, the reduction of broadband noise component from the compressor, due to the interaction of laminar and turbulent flows with blades, has remained a challenging task and is also believed to play a significant role in the overall engine noise [1]. One of the sources of radiated noise from the aero-engine fan and airframe is trailing-edge noise.

The use of passive flow control methods for reducing airfoil noise has been the subject of much research. In particular, trailing- and leading-edge serrations of airfoils have received the maximum attention [2-12]. It has been shown analytically [2, 3] and experimentally [4-10] that the use of trailing- and leading-edge serrations can lead to significant noise reduction in airfoils over a wide range of frequencies. In recent studies, Gruber *et al* [3-6]. Experimentally studied airfoil trailing-edge noise reduction by applying different types of trailing-edge serrations. Three serrated-type trailing-edges were designed, namely as slots, sawtooth and slotted-sawtooth. A random trailing-edge geometry aimed at reducing the scattering efficiency at the trailing-edge has also been considered. All serrations are made of cardboard of 0.8mm thickness and tested on a NACA65(12)-10 airfoil in an open jet wind tunnel. Results had shown that broadband noise reductions of up to 5dB can be obtained using the slotted-sawtooth and up to 3dB with the random trailing-edge serration. More importantly, with these two trailing-edges, the expected high frequency noise increment, which is normally observed with sawtooth serrations, is reduced to almost zero with the slotted sawtooth. It has been suggested these slotted trailing-edge serrations are suitable to be applied to low speed fans, such as wind turbine blades. Although the aeroacoustic performance of trailing- and leading-edges has been studied extensively in recent years, no proper study has been carried out on the aerodynamic performance of such passive edge treatments. This paper focuses on the aerodynamic performance of serrated trailing-edges on airfoils. Aerodynamic lift and drag measurements has been carried out for symmetric and asymmetric airfoils over a wide range of Reynolds number and angles of attack. To better understand the underlying physics of noise reduction and development of the wake of airfoil with serrations, two-dimensional Laser Doppler Anemometry (LDA) measurements and hot-wire measurements were carried out.

II. Experiments and Facilities

A. Wind Tunnel Facility

1) Force Measurements

The aerodynamic force (lift and drag) measurements were carried out in the University of Bristol's closed return wind tunnel. It has an octagonal working section with a width W = 2.1 *m* and height H = 1.5 *m* and is capable of producing a stable velocity in the range of 10 *m/s* to 60 *m/s.* A schematic of the wind tunnel test section, the airfoil with circular endplates (diameter D = 0.34 *m*) and the force balance system is shown in Figure 1(a). The experimental setup for NACA 65(12)-10 with serrated trailing-edge is show in Figure 1 (b). An AMTI OR6-7-2000 force balance was used for measurement of the aerodynamic forces. The voltage induced from the force balance passes through an AMTI MSA-6 strain gauge amplifier and is converted into data using a control system built in LabVIEW system design software. Data independency tests have been carried at different sampling frequencies and it has been established that the sampling frequency of 37 *Hz* provided the best data independency and least uncertainty. Three sets of data were collected for a time period of 10 seconds.

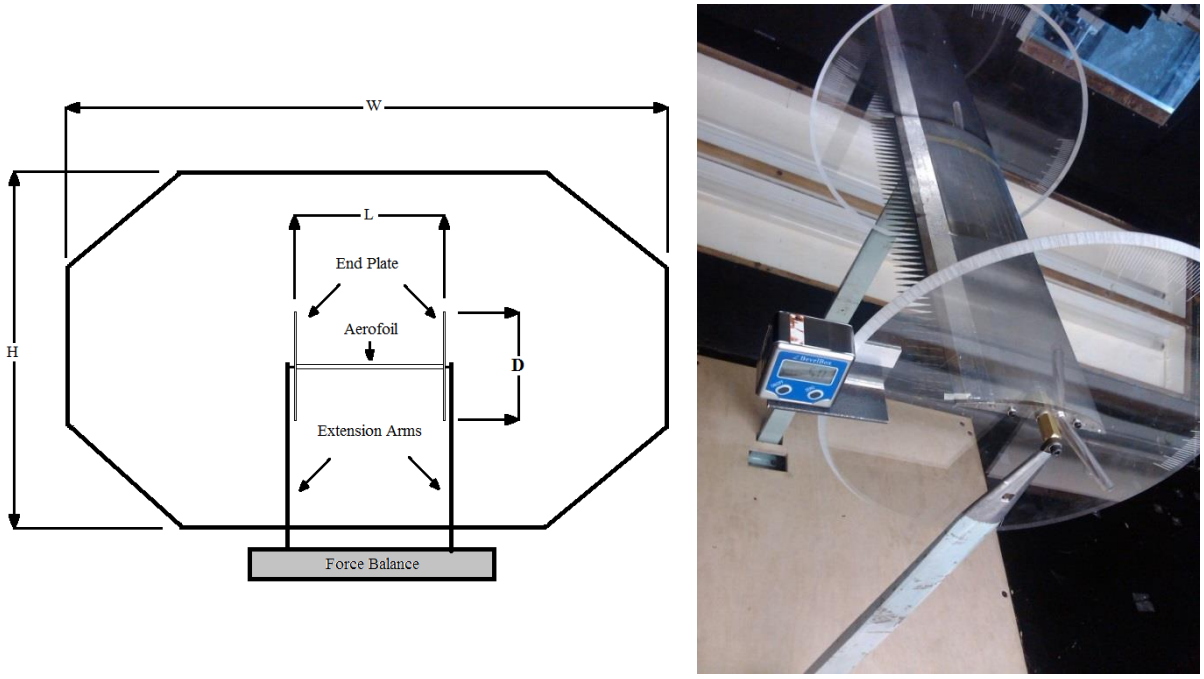

(a) (b)

Figure 1. Wind tunnel setup for force measurement. *(a) Cross section sketch of wind tunnel setup. (b) Experimental setup with NACA 65(12)-10.*

2) Flow measurements

The two-dimensional LDA measurements were carried out in the closed return low turbulence wind tunnel at the University of Bristol. It has an octagonal test section with a width $W_{LT} = 0.8\ m$ and height $H_{LT} = 0.6\ m$ and is capable of producing a minimum reliable speed of 10 *m/s* and a maximum speed of 100 *m/s*. Data was acquired using the Dantec Dynamics Stabilite 2016 LDA system and BSA flow software. In order to better understand the wake development and the energy content of the turbulence structures within the wake, several hotwire measurements have also been performed. Hot-wire measurements were carried out in the open jet wind tunnel at the University of Bristol. It has an circular nozzle exit with a radius $R_n = 1.1\ m$ and is capable of producing a minimum reliable speed of 10 *m/s* and a maximum reliable speed of 30 *m/s*. Data were acquired with constant temperature single hot-wire probe Dantec 55P16 that has a 5 μm diameter and 1.2 *mm* long platinum-plated tungsten wire sensor, it was connected to an analog-digital Dantec StreamWare ProV5.14 for calibration the probe and acquiring the data.

B. Airfoil models

In order to carry out a comprehensive study, the aerodynamic performance for two airfoils have been investigated using a symmetrical NACA 0012 and a cambered asymmetrical NACA 65(12)-10 airfoil. The airfoils were manufactured using ProLab composite material and machined using a computer numerical control (CNC) machine. Both the airfoils have 1 *mm* blunt trailing-edge with a 15 *mm* deep and 0.8 *mm* thick slot cut through the trailing-edge along the span in order to allow flat plate serration inserts to be fitted to the airfoil, as shown in Fig. 2.

The Baseline 1 airfoil shown in Figure 2 (c) and (d) is composed of a main body with a chord length of $C = 0.14\ m$ and span length of $L = 0.45\ m$ along with the slit at the trailing-edge with no flat plate inserts. The Baseline 2 airfoil shown Figure 2 (c) and (d) is the Baseline 1 airfoil with a flat plate inserts with no-serrations at the trailing-edge effectively increasing its chord length to $C = 0.155\ m$ and having the same span length of $L = 0.45\ m$.

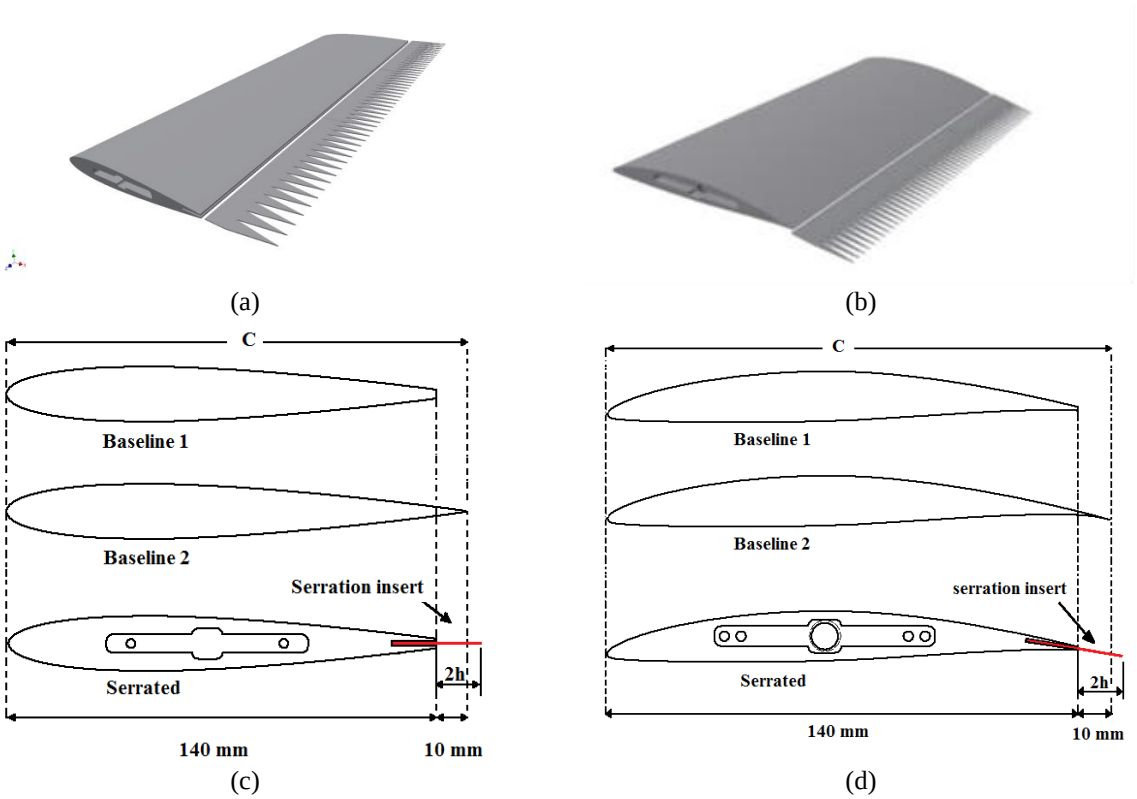

Figure 2. Trailing-edge treatment model *(a) CAD assembly view of NACA 0012 with trailing-edge serrations. (b) CAD assembly view of NACA 65(12)-10 with trailing-edge serration. (c) NACA 0012 with and without trailing-edge serrations (d) NACA 65(12)-10 with and without trailing-edge serrations*

Based on previous analytical and experimental results of noise reduction effects using trailing-edge serrations [2-6], two types of serrations with good noise reduction performance were selected for the aerodynamic study. The two types of serrations were *sawtooth serrations* and *slotted-sawtooth serrations*. As shown in Fig. 3 and Table 1, seven serrations with different geometrical parameters (amplitude $2h$, periodicity wavelength λ, angle of serration edge α_S, slot width d and slot depth H) were used for detailed aerodynamic performance measurements. There is no consensus in the literature on how to define and apply serrations to airfoils. Many researcher have applied serrations as a simple flap to an existing airfoils and therefore increasing airfoil's surface area, while some other [6] tried to keep the surface area constant. In order to understand the effects of both treatment, in these study we have considered two Baseline cases. As shown in Fig. 2, Baseline 1 airfoil uses the serrations as an additional flap configuration (thus increasing the airfoil surface area), whereas the Baseline 2 airfoil is designed in such a way to have the same surface area as the serrated airfoil.

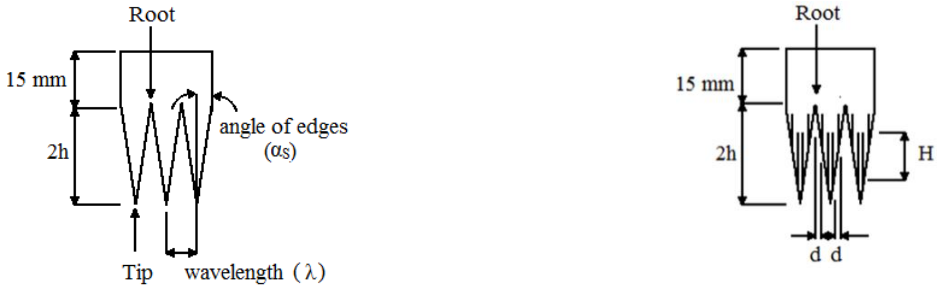

Figure 3. Trailing-edge treatment model *(a) Sawtooth serration (b) Slotted-sawtooth serration*

Table 1 Geometrical parameters of trailing-edge serrations

Cases	Serration types	$2h$	λ	λ/h	α_S	d	H
		mm	mm		degrees	mm	mm
Case 1	Baseline 1	0	-	-	-	-	-
Case 2	Baseline 2	15	-	-	-	-	-
Case 3	sawtooth	30	3	0.2	2.86	-	-
Case 4	sawtooth	30	9	0.6	8.53	-	-
Case 5	sawtooth	30	22.5	1.5	45	-	-
Case 6	slotted-sawtooth	30	9	0.6	8.53	0.5	15
Case 7	slotted-sawtooth	30	9	0.6	8.53	0.5	5

III. Results and Discussion

A. Lift and Drag Coefficients

The lift and drag measurements of NACA 0012 and NACA 65(12)-10 airfoils with trailing-edge serrations are presented and discussed in this section. Even though the wind tunnel experiments were carried out for a wide range of chord-based Reynolds number $Re_c = 2 \times 10^5$ to 6×10^5, corresponding to flow velocity of $U = 20\, m/s$ to $60\, m/s$, results are only presented for $Re_c = 3 \times 10^5$ and 5×10^5 (i.e. $U = 30\, m/s$ and $50\, m/s$). The NACA 0012 and NACA 65(12)-10 airfoils have been tested over a wide range of angles of attack (AoA) from 0° to $20^\circ$and -5° to 20°, respectively. These AoA ranges include the relevant angles covered in the prior research on trailing-edge noise [4-6, 9-12] and also the stall regions.

1) NACA 65(12)-10 aerodynamic force measurements

The lift and drag coefficients results for NACA 65(12)-10 airfoil without (Baseline 1) and with (Baseline 2) the trailing-edge serration are presented in Fig. 4. The upper two plots shows the results for the three different sawtooth serrations with wavelengths of $\lambda = 3\ mm$, $9\ mm$ and $22\ mm$ and amplitude of $2h = 30\ mm$. The bottom two plots show the results for the slotted-sawtooth serrations with a wavelength of $\lambda = 9\ mm$ and amplitude of $2h = 30\ mm$. The slots have a width of $d = 0.5\ mm$, and depths of $H = 5\ mm$ and $15\ mm$.

The results in Fig. 4 have shown that for both the wind speeds presented in this study, the lift coefficient reduces up to 15% over AoA range of -5° to about 10° for the NACA 65(12)-10 airfoil fitted with sawtooth serrations in comparison with the Baseline 2 (i.e. constant surface area). Result comparison between Baseline 1 (no trailing-edge insert) and Baseline 2 (flat-plate trailing-edge insert) shows a prominent increase in lift coefficient with Baseline 2 due to the increased surface area. Results have also shown that the trailing-edge serrations increase the lift coefficient in the pre-stall region but do not particularly change the stall behavior ($C_L - AoA$ curves) of the airfoil. However, in comparison with Baseline 1, the lift coefficient of the serrated airfoils shows a significant increase over the whole range of AoAs. For angles of attack larger than 10°, the drag coefficient of serrated trailing-edge is higher than that of the Baseline cases and it can also be observed form the results that the serrations with larger wavelengths produce more drag. The lift coefficient results for NACA 65(12)-10 airfoil fitted with slotted-sawtooth serrations show a reduction of up to 30% in comparison with Baseline 2 over the entire range of AoAs and the maximum reduction is found at small angle of attack region. Again, these results show an increase over the whole range of AoAs compared with Baseline 1.

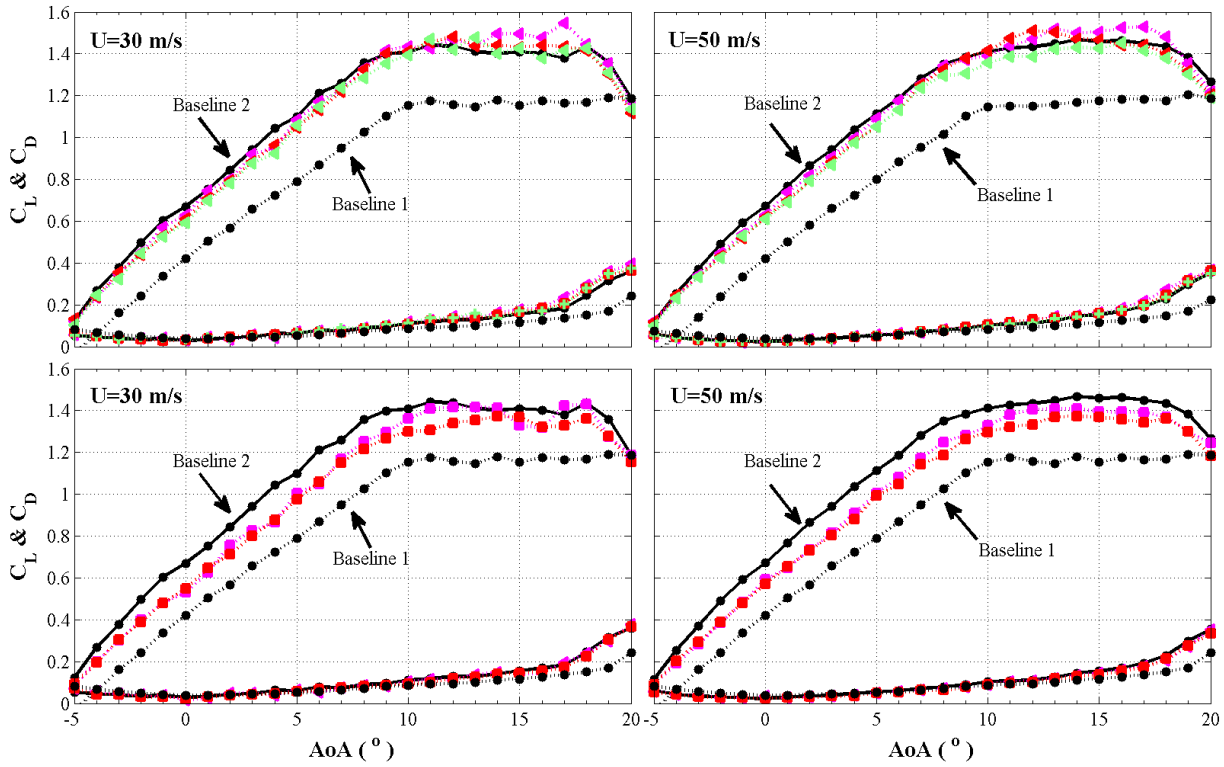

Figure 4. Lift and drag coefficient results for NACA 65(12)-10 fitted with different serrations *(a) sawtooth serrations. Triangles: Red: $\lambda = 22.5\ mm$; Pluses: $\lambda = 9\ mm$; Green: $\lambda = 3\ mm$. (b) slotted-sawtooth serrations ($\lambda = 9\ mm, 2h = 30mm, d = 0.5\ mm$). Square: Pluses: H= 5 mm; Red: H= 15 mm.*

2) NACA 0012 aerodynamic force measurements

The lift and drag coefficient results for the NACA 0012 airfoil fitted with different trailing-edge sawtooth serrations ($\lambda = 3\ mm$ and $9\ mm$; amplitude of $2h = 30\ mm$) and slotted-sawtooth serrations ($\lambda = 9\ mm$, $2h = 30\ mm$, $d = 0.5\ mm$ $H = 5\ mm$ and $15\ mm$), at tested wind speeds of $U = 30\ m/s$ and $50\ m/s$ and over the angle of attack range of 0° to 20° are presented in Fig. 5. The lift coefficient results show that the behavior of symmetric NACA0012 airfoil is noticeably different to that of the asymmetric NACA 65(12)-10 especially at low angles of attack, as seen in Figs. 4 and 5. The effect of serrations on NACA 0012 lift coefficient is less significant compared to that of NACA 65(12)-10, particularly at lower speeds. Serrations significantly affect the maximum lift coefficient ($C_{L,max}$) over the critical AoA ranges from 12° to 15°, but it appears to show improvement in the lift performance at deep stall angles from 17° to 20°. The drag of NACA 0012 airfoil with serrations is generally lower than that of the Baseline 2. However, over the critical angle region and deep stall region an increase in the maximum lift coefficient is observed with sawtooth serration in comparison with Baseline 1. This increase is less significant for the slotted-sawtooth serrations. As mentioned earlier, based on previous analytical and experimental results in [2-6], sharp sawtooth (small α_s) and slotted-sawtooth serrations provide large and robust noise reduction over a wide frequency range. The aerodynamic results presented here, however, have revealed that such effective trailing-edge treatment (in term of noise) are prone to significant aerodynamic losses.

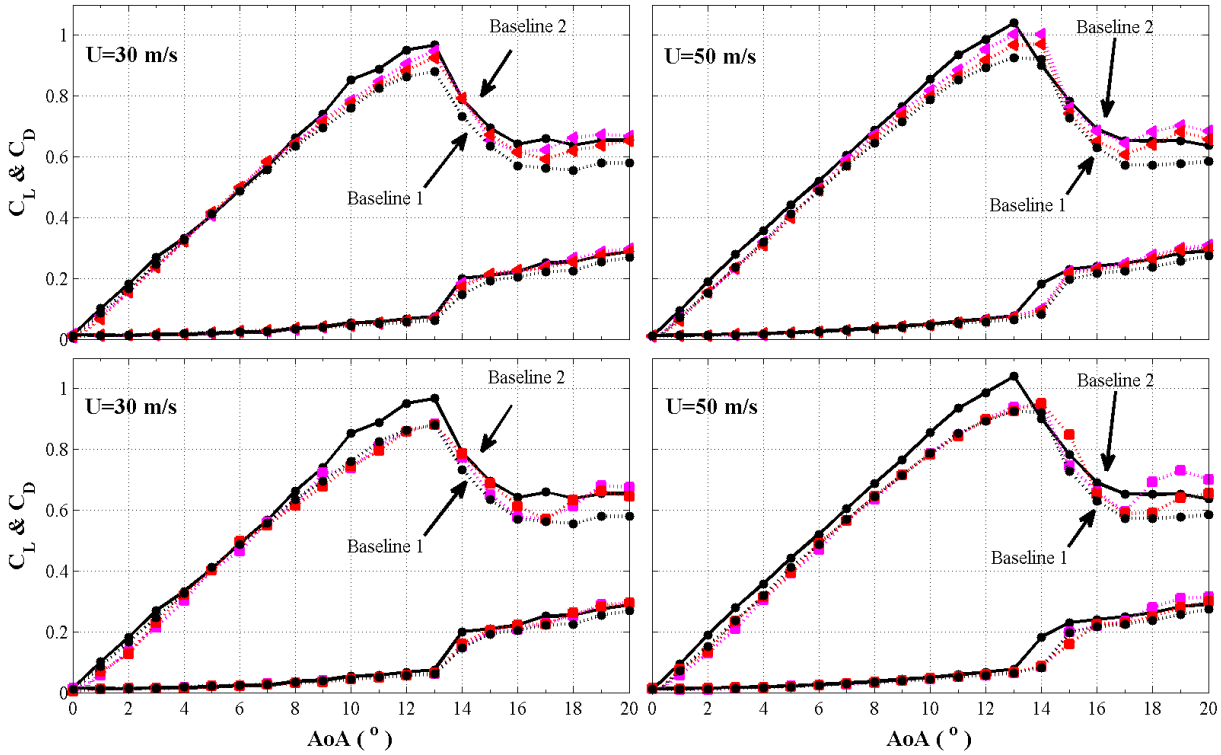

Figure 5. Lift and drag coefficients for a NACA 0012 airfoil fitted with different serrations. *Triangles: $\lambda = 9$ mm; squares: sawtooth serration with $\lambda = 3$ mm wavelength; pluses: slotted-sawtooth serration with $\lambda = 9$ mm, $d = 0.5$ mm and $H = 5$ mm; stars: slotted-sawtooth serration with $\lambda = 9$ mm, $d = 0.5$ mm and $H = 15$ mm.*

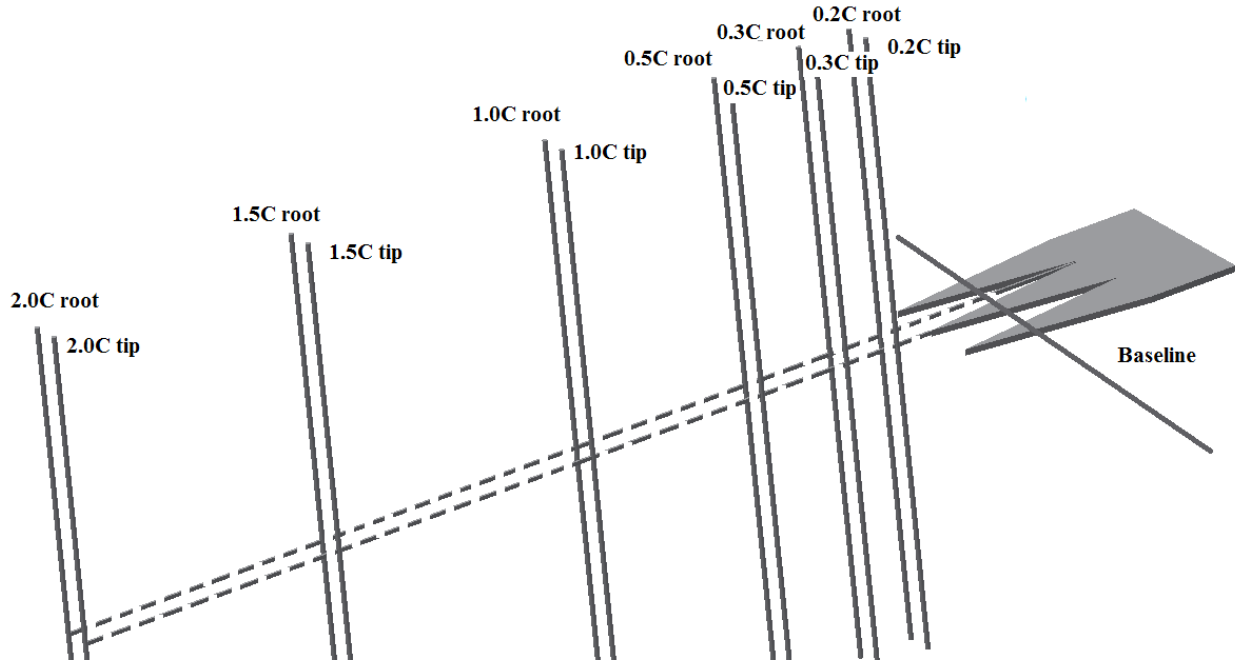

Figure 6. Chord-wise locations used along the tip and root of the serration for LDA measurements.

B. Wake profiles

To better understand the effect of the serration on the aerodynamic performance of airfoils and also the flow field in the wake region several LDA measurements have been carried out. The wake development of NACA 65(12)-10 airfoils with and without serration (Baseline 2) measured using LDA are discussed in this section. Wind tunnel experiments have been carried out for a chord-based Reynolds number of $Re_c = 3 \times 10^5$, corresponding to flow velocity of $U_0 = 30\ m/s$. The NACA 65(12)-10 airfoil was tested for angles of attack (AoA) 0°, 5°, 10° and 15°. The wake measurements were logged at downstream locations 0.2C, 0.3C , 0.5C , 1.0C , 1.5C , 2.0C, relative to the trailing-edge of the Baseline 2 airfoil. Each measurement line, shown in Fig. 6, has been populated with 60 points to properly capture the wake behavior. Results are presented for airfoil trailing-edges with no-serration (Baseline 2), sawtooth serration ($\lambda = 9\ mm$) and slotted-sawtooth serration $\lambda = 9\ mm$, $d = 0.5\ mm$ and $H = 15\ mm$) at angles of attack, AoA 0° and 10°.

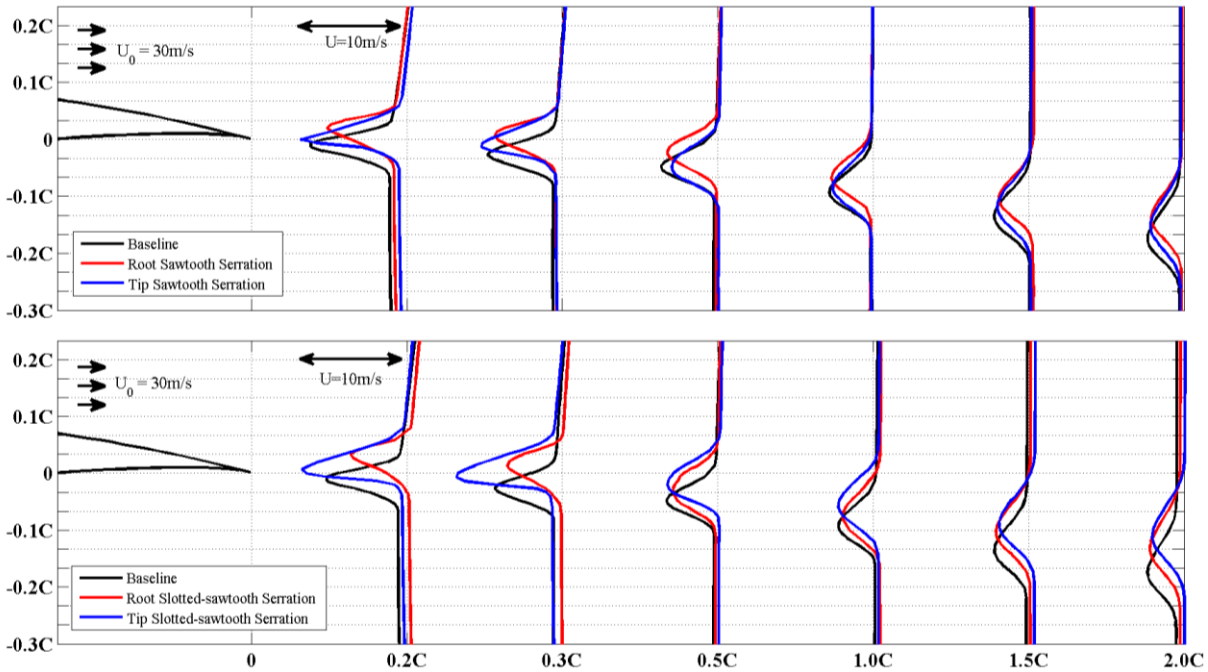

Figure 7. Wake profile for serrated NACA 65(12)-10 airfoil at AoA $= 0^\circ$ and $U_0 = 30$ m/s. *Black line: baseline 2; Red line:root location ; Red line: tip location*

Figures 7 and 8 present the wake velocity profiles for the untreated (Baseline 2) and treated NACA 65(12)-10 airfoil (sawtooth and slotted-sawtooth) at the tip and root locations, as shown in Fig. 6. at AoA $= 0^\circ$ and 10°, respectively. From the wake profile results at 0° angle of attack in Fig. 7, it can be observed that the wake location, the peak and the magnitude in particular can change significantly by the serrations. It can also be seen that the velocity profiles at the root locations are very different from those at the tip locations. This can cause significant shear stress between the tip and root planes. It is also clear from the results that the wake profile at the root location has moved upwards, relative to the baseline and the tip results, which is an indication of a jet flow originating at the root and moving upwards within the serration valleys. The wake magnitude for the slotted-sawtooth serration is considerably lower for the tip and significantly higher for the root compared to the Baseline and sawtooth serration cases at downstream locations 0.2C and 0.3C. The wake turning (downwash) angle for both the sawtooth and slotted-sawtooth serration is much less than that of the Baseline case. The difference in peak location between the tip and root wake for both the sawtooth and slotted sawtooth serration is about 0.025C closer to the trailing-edge locations at 0.2C and 0.3C, this difference gradually reduces as the flow moves further downstream. This might be due the difference in the effective distance of the wake locations from the actual trailing-edge point for both the tip and root and possible three-dimensional effects. The reduction in turning angle for the serrated airfoils in comparison with the Baseline will result in a slight loss of lift produced from the downwash of the airfoil, as demonstrated earlier in Figs. 4 and 5.

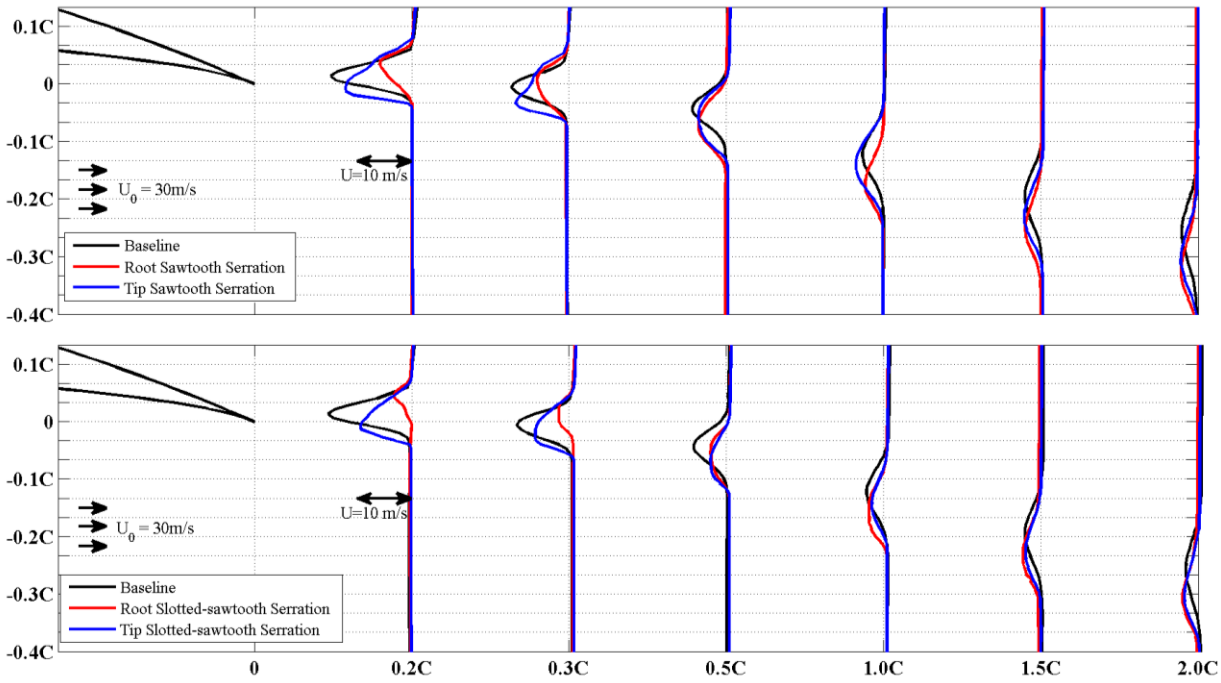

Figure 8. Wake profile for serrated NACA 65(12)-10 airfoil at $\mathbf{AoA} = \mathbf{10}^{\circ}$ and $\boldsymbol{U_0} = \mathbf{30\ m/s}$. *Black line: baseline 2; Red line: root location ; Red line: tip location*

The wake profile results at angle of attack of 10°, Fig. 8, shows that both the sawtooth and slotted-sawtooth serrated airfoils behave quite similarly. The peak amplitude location of the wake for both the sawtooth and the slotted-sawtooth tip location appears to be slightly lower than that of the Baseline, while that of the root has a significant reduction of up to 60% for sawtooth serration and up to 80% for slotted-sawtooth serration at 0.2C. The downwash angle for both the sawtooth and slotted-sawtooth tip location appears to be larger than that of the Baseline. It can also be seen that the turning angle and the magnitude of the root has significantly reduced for the 0.2C and 0.3C locations compared with the Baseline and tip for both the serrations at high angles of attack as the flow passes through the serration valleys at higher angle of attacks reenergizing the flow. The turning angle is higher than that of the Baseline for both the serrations for downstream locations from 0.5C to 2.0C.

The turbulent kinetic energy (TKE) results for NACA 65(12)-10 airfoils, with (sawtooth and slotted-sawtooth) and without treatment (Baseline 2), at $\mathrm{AoA} = 0^{\circ}$ and 10° are presented in Figs. 9 and 10, respectively. Results have shown that the peak amplitude for the normalized TKE at the tip and root locations has slightly decreased compared to that of the baseline. It can also be seen that the use of serrations lead to wider wakes. The TKE magnitude for the slotted-sawtooth serration tip is noticeably different from that of the sawtooth serration tip as it has a double peak, with an evident difference between the turbulence level on the upper and lower end of the wake width.

At higher angles of attack the results of the normalize TKE between the sawtooth serrations and slotted-sawtooth serrations are significantly different, see Fig. 10. The TKE maximum amplitude for both types of serrations, at tip and root locations, are significantly smaller than the baseline result, i.e. up to 30% reduction for the sawtooth serration and about 70% reduction for the slotted sawtooth. The higher level of turbulence dissipation for the slotted-sawtooth serration is believed to be due to the flow three dimensionality and the shear stress acting between the tip and root planes. Further investigation is necessary to determine the amount of the energy dissipation as a result of the inter-plane interactions. Results have also shown that the turbulence level decay much faster for both serration cases at further downstream locations, and that the slotted-sawtooth case shows a much quicker turbulence decay than the sawtooth case.

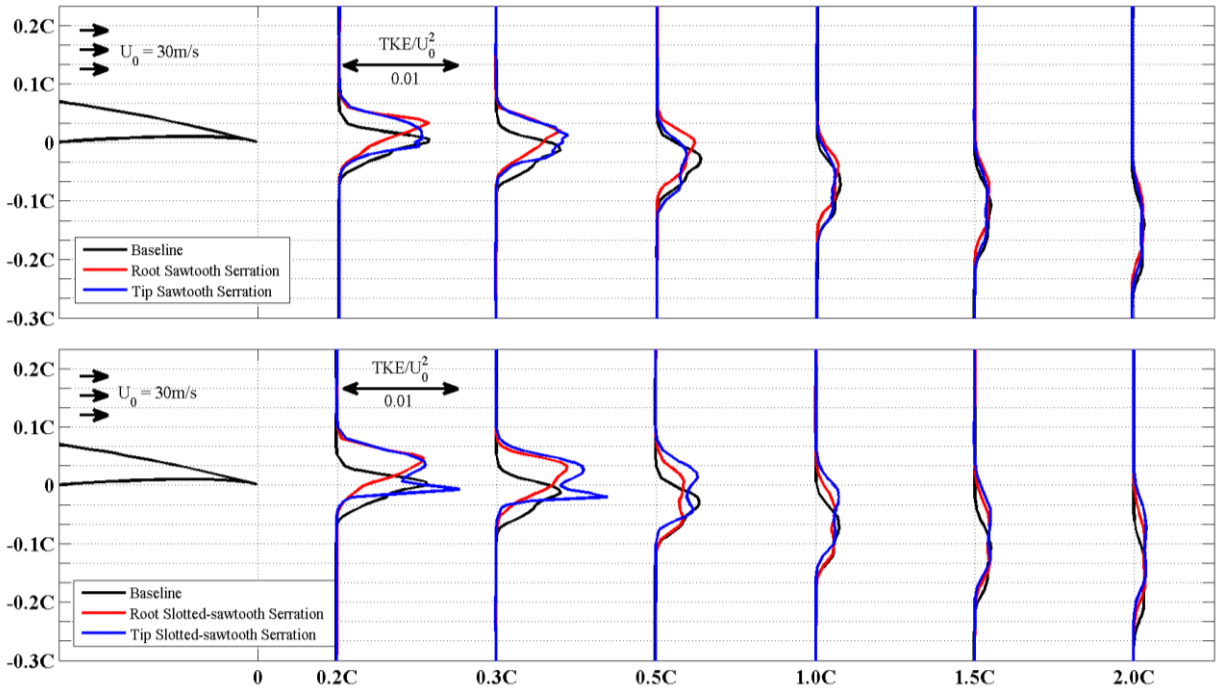

Figure 10. TKE for serrated NACA 65(12)-10 airfoil at $\mathbf{AoA} = \mathbf{0}^{\circ}$ and $\boldsymbol{U_0} = \mathbf{30\ m/s}$. *Black line: baseline 2; Red line:root location ; Red line: tip location*

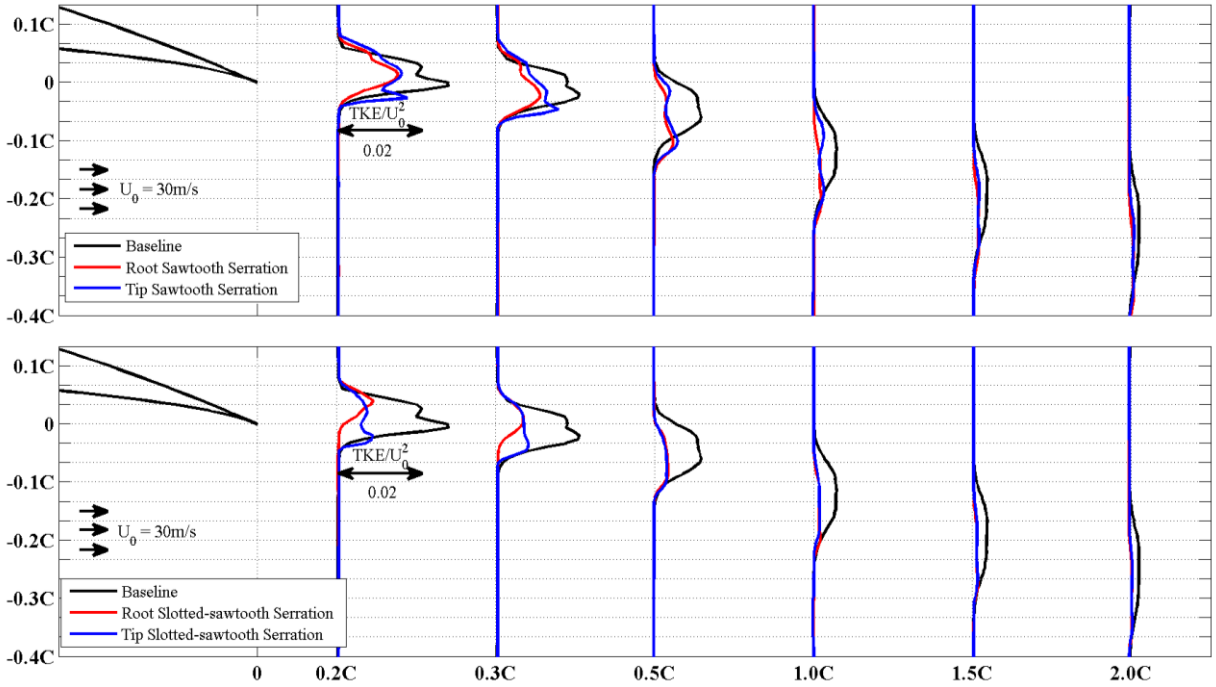

Figure 10. TKE for serrated NACA 65(12)-10 airfoil at $\mathbf{AoA} = \mathbf{10}^{\circ}$ and $\boldsymbol{U_0} = \mathbf{30\ m/s}$. *Black line: baseline 2; Red line:root location ; Red line: tip location*

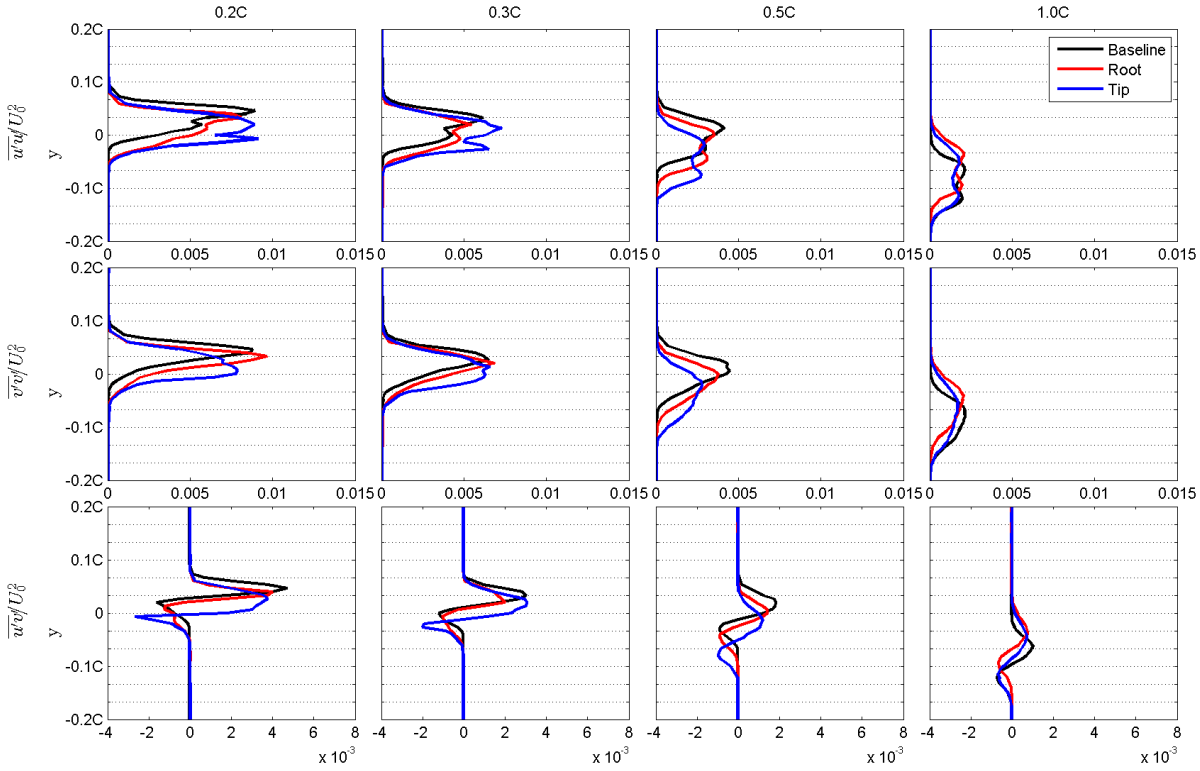

Figure 11. Reynolds stress components profiles for sawtooth serrated NACA 65(12)-10 airfoil at AoA = 0° and U_0 = 30 m/s. *Black line: baseline 2; Red line:root location ; Red line: tip location*

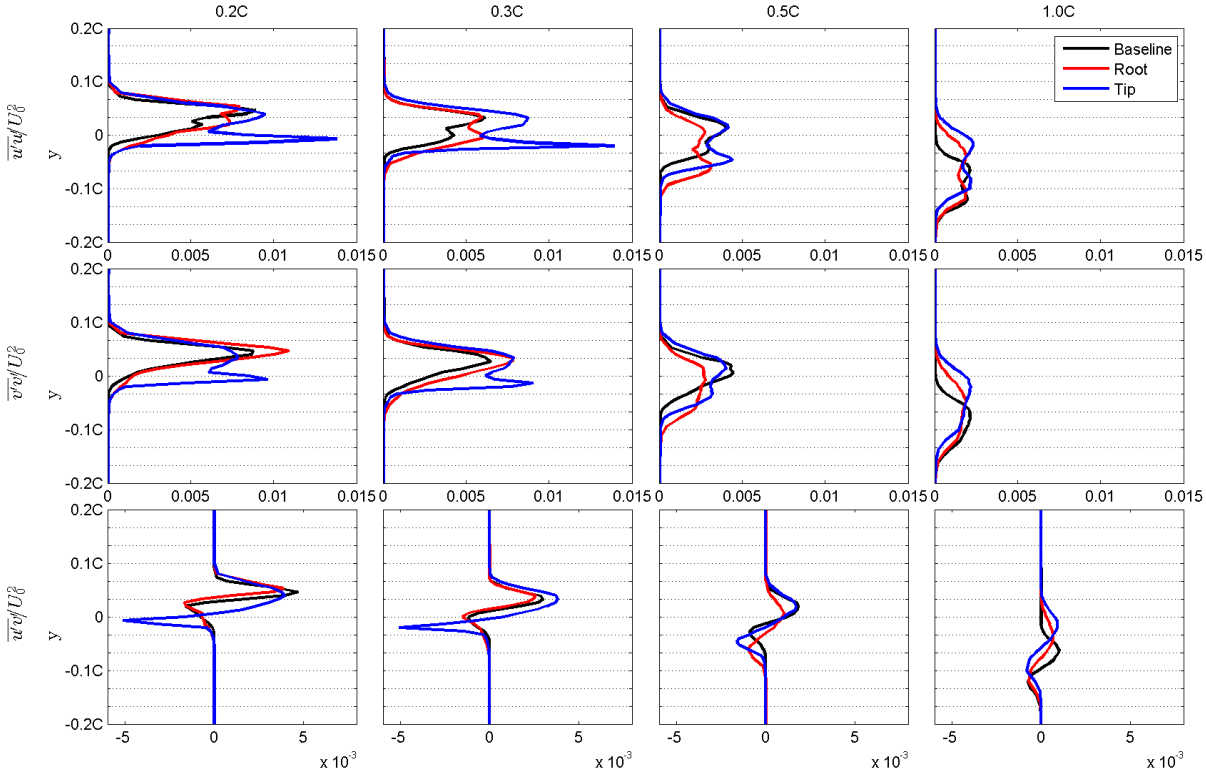

Figure 12. Reynolds stress components profiles for slotted-sawtooth serrated NACA 65(12)-10 airfoil at AoA = 0° and U_0 = 30 m/s. *Black line: baseline 2; Red line:root location ; Red line: tip location*

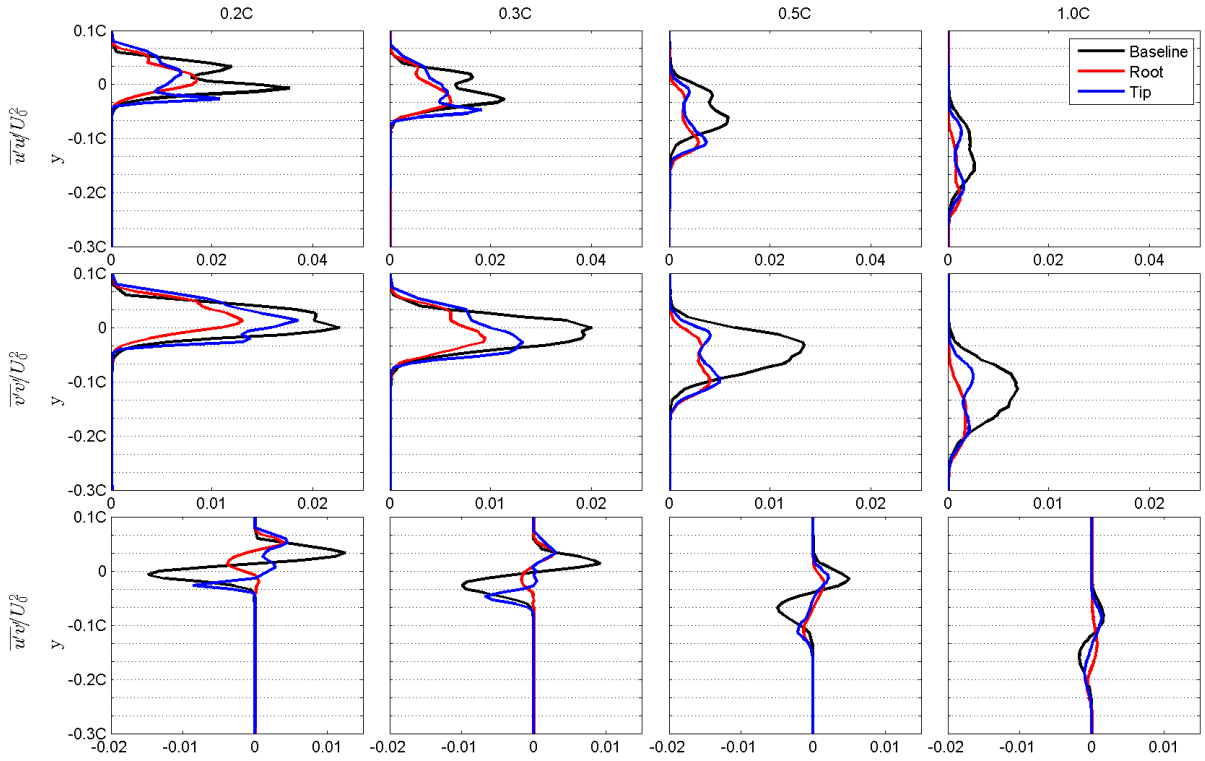

Figure 13. Reynolds stress components profiles for sawtooth serrated NACA 65(12)-10 airfoil at AoA = 10° and $U_0 = 30$ m/s. *Black line: baseline 2; Red line:root location ; Red line: tip location*

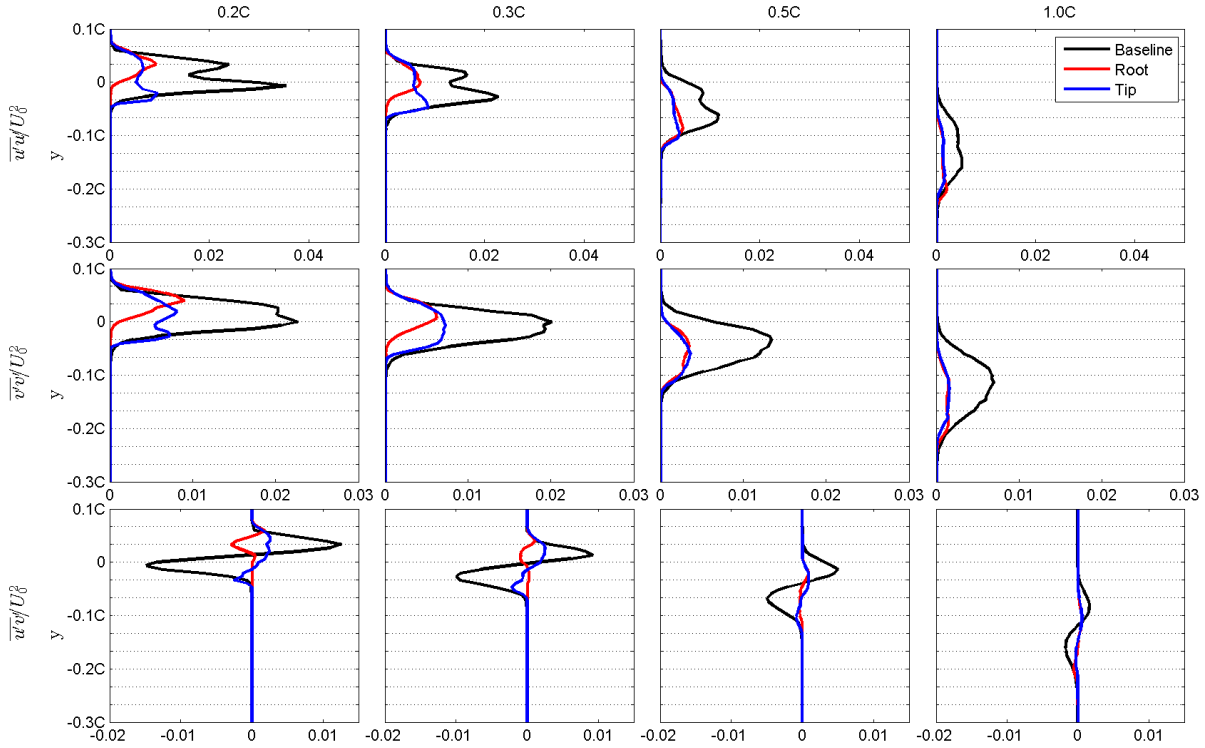

Figure 14. Reynolds stress components profiles for slotted-sawtooth serrated NACA 65(12)-10 airfoil at AoA = 10° and $U_0 = 30$ m/s. *Black line: baseline 2; Red line:root location ; Red line: tip location*

Understanding the underlying physics of the changes to the wake development as a result of using serration requires more in-depth turbulence studies. Figures 11 to 14 present the results for the normal ($\overline{u'u'}/U_0^2$, $\overline{v'v'}/U_0^2$) and shear $\overline{u'v'}/U_0^2$ stress components. Results are presented at different the downstream location (0.2C, 0.3C, 0.5C and 1.0C) and at AoA $= 0^\circ$ and 10°. From Figs. 11 to 14 at AoA $= 0^\circ$ and AoA $= 10^\circ$, the $\overline{u'u'}/U_0^2$, $\overline{v'v'}/U_0^2$ stress components for the sawtooth and slotted-sawtooth serrations, at the tip and root locations, show similar trends to those of the TKE seen in Figs. 9 and 10. The similarity of the normal stearmwise and spanwise stresses, *i.e.* $\overline{u'u'}$ and $\overline{v'v'}$, suggests that the flow within the wake region is nearly isotropic. Results have also shown that the Reynolds shear stress $\overline{u'v'}$, generally decreases as a result of the serrations. Knowing that the shear stress magnitude determines the amount of turbulence production rate within the wake area ($P = -\overline{u'v'}\,\partial U/\partial x$), one can conclude that serrations decrease the TKE by reducing the shear stress. This might be due to the interactions between the flows through the serration valley and flow from the serration tip. This issue requires more investigation.

C. Hotwire measurement for wake profile

The turbulence energy content of the turbulent structures within the wake of the NACA 65(12)-10 airfoil, with and without serrations, has been studied. The velocity power spectral density (PSD) results have been measured using hotwire at the chord-based Reynolds number of $Re_c = 2 \times 10^5$, corresponding to the flow velocity of $U_0 = 20\ \mathrm{m/s}$, and at angles of attack of 0° and 10°. The data was collected with a sampling frequency of 40 kHz and sampling time of 10 seconds. The data has been acquired at two downstream locations, 0.2C and 0.5C. Results presented in Fig. 15 to 19 are the PSD contour plots for serrated airfoils, normalized with the results from the untreated airfoil (Baseline 2). In Figs. 15 and 16 for AoA $= 0^\circ$, it can be seen that serrations can lead to an increase in the energy content of the turbulent structure below the chord-line, particularly around $f = 50Hz$ and $3000Hz$. Results also show that energy content of turbulent structure above the chord-line decreases significantly compared with the Baseline 2. However, compared with sawtooth serration cases, the slotted-sawtooth cases show a significant change in power reduction for the turbulent structures above the chord line, especially for the root locations. Figures 17 and 18 show the normalized velocity PSD results for the NACA 65(12)-10 at AoA $= 10^\circ$. It can be seen that the areas greatly affected due to the serrations are much smaller than those in Figs. 15 and 16 and are confined within small y-regions and appear at relatively higher frequencies.

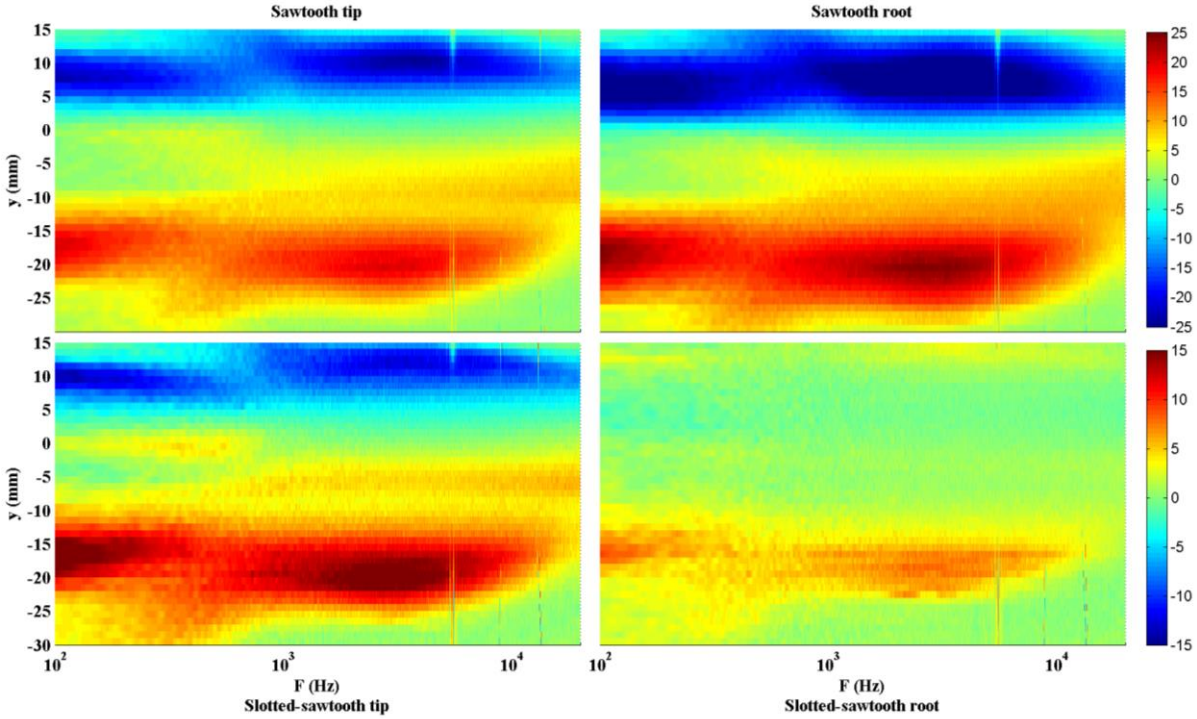

Figure 15. Normalized velocity power spectral density (PSD) contour plots of serrated NACA 65(12)-10 airfoil normalized with Baseline 2 airfoil at AoA $= 0^\circ$ and $U_0 = 20\ \mathrm{m/s}$ at downstream location 0.2C.

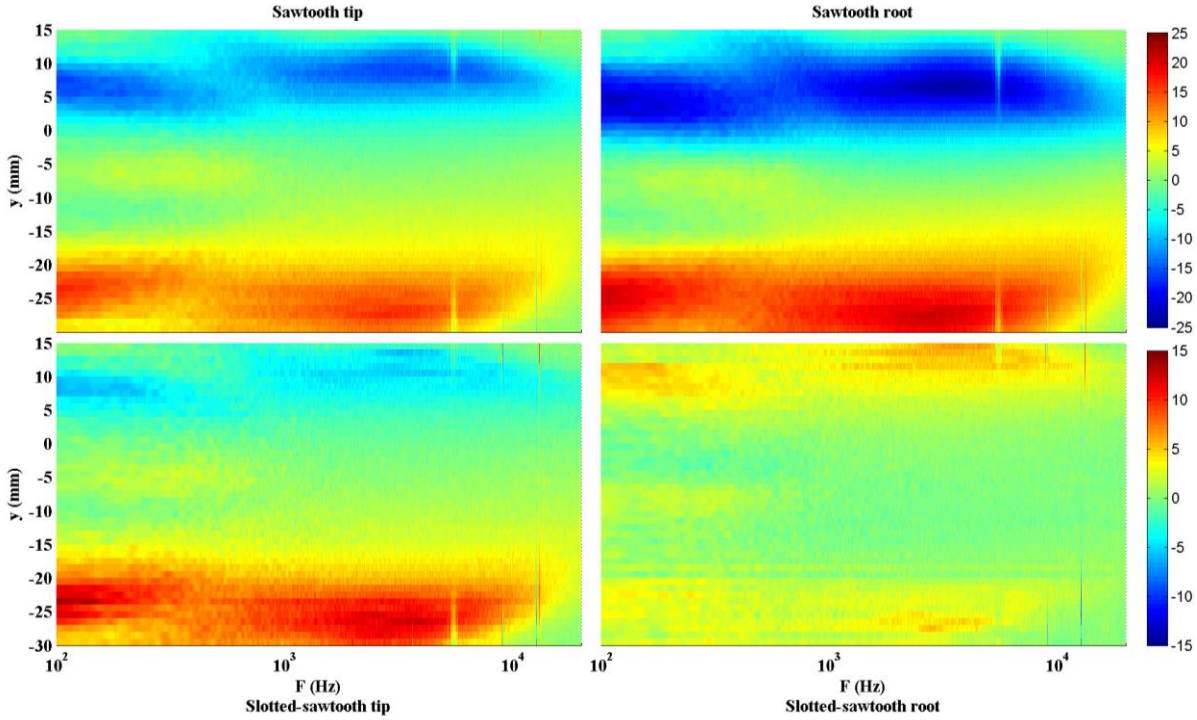

Figure 16. Normalized velocity power spectral density (PSD) contour plots of serrated NACA 65(12)-10 airfoil normalized with Baseline 2 airfoil at $\mathbf{AoA} = 0^{\circ}$ and $U_0 = 20$ m/s at downstream location 0.5C.

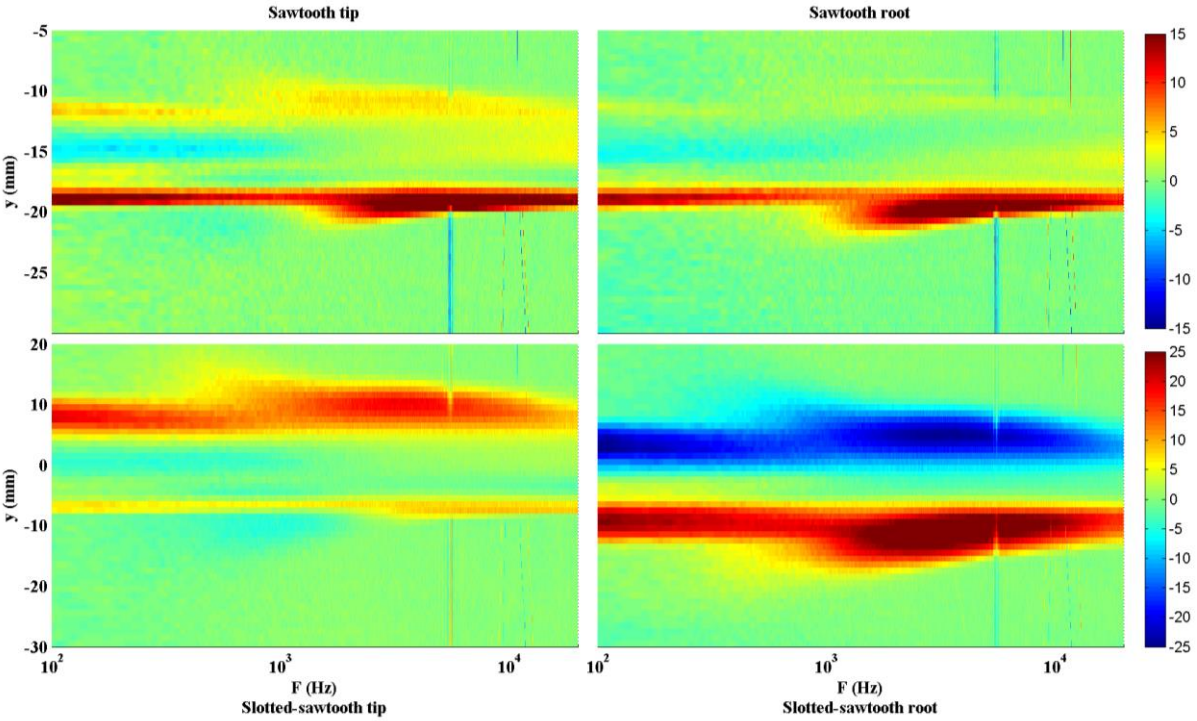

Figure 17. Normalized velocity power spectral density (PSD) contour plots of serrated NACA 65(12)-10 airfoil normalized with Baseline 2 airfoil at $\mathbf{AoA} = 10^{\circ}$ and $U_0 = 20$ m/s at downstream location 0.2C.

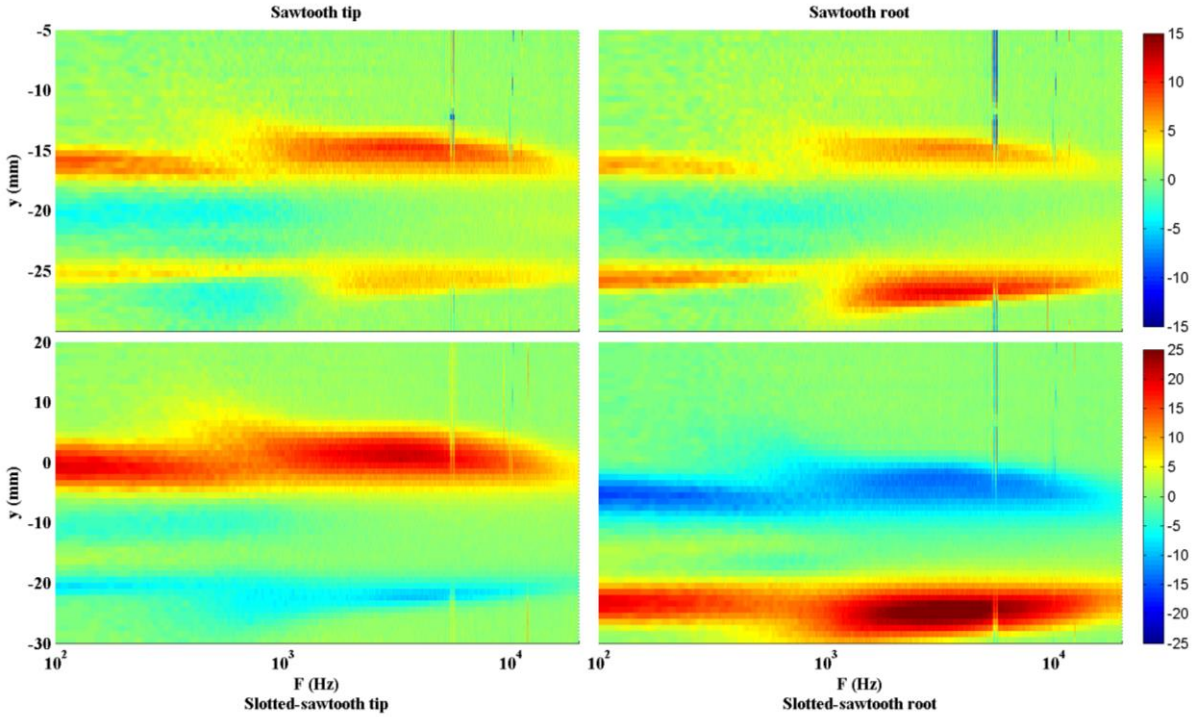

Normalized velocity power spectral density (PSD) contour plots of serrated NACA 65(12)-10 airfoil normalized with Baseline 2 airfoil at $\mathbf{AoA} = \mathbf{10}^{\circ}$ and $\boldsymbol{U_0} = \mathbf{20\ m/s}$ at downstream location 0.5C.

IV. Conclusion

The aerodynamic and aeroacoustic performance of airfoils fitted with trailing-edge serrations has been studied. Prior studies had shown that such treatments could significantly reduce the trailing edge noise. However, the results in this paper show that the trailing-edge serrations can also significantly change the aerodynamic performance of the airfoil. It has been shown that the level of the aerodynamic performance changes depends on the type of the airfoil, as well as the geometrical characteristics of the serration. Results have shown that while serrations do not particularly change the overall shape of the C_L-α curves and the stall properties of the airfoil, they can significantly reduce the lift coefficient. The wake velocity, turbulence and energy content of the turbulence structures within the wake region have also been studied. Results have shown that serrations can significantly change the shape of the wake profile and the location of high turbulence areas within the wake region. It has also been observed that serrations generally decrease the energy content of the turbulent structures within the wake and above the chord-line and significantly increase the energy content of the coherent turbulent structures below the chord-line at some particular frequencies.

References

1 Hardin, J. C., "Airframe self-nosie - four years research", NASA Tech Memo, 1976.

2 Howe, M. S., "Noise produced by a sawtooth trailing-edge", *Journal of the Acoustical Society of America*, Vol. 90 No. 1, pp. 482–487, 1991.

3 Azarpeyvand, M., Gruber, M., Joseph, P. F., "An Analytical Investigation of Trailing-edge Noise Reduction Using Novel Serrations", *19th AIAA/CEAS Aeroacoustics Conference*, May 2013.

4 Gruber, M., Joseph, P. F., Azarpeyvand, M., "An experimental investigation of novel trailing-edge geometries on airfoil trailing-edge noise reduction", *19th AIAA/CEAS Aeroacoustics Conference*, 2013.

5 Gruber, M., Azarpeyvand, M., and Joseph, P. F., "Airfoil trailing-edge noise reduction by the introduction of sawtooth and slitted trailing-edge geometries", *20th International Congress on Acoustics*, Sydney, Australia, 23 – 27, August 2010.

6 Gruber, M., *Aerofoil noise reduction by edge treatments*, Doctoral Thesis, University of Southampton, Faculty of Engineering and the Environment, 2012.

7 Oerlemans, S., Fisher, M., Maeder, T. and Kögler. K., "Reduction of wind turbine noise using optimized aerofoils and trailing-edge serrations". *AIAA journal*, Vol. 47, pp.1470 – 1481, 2009.

8 Moreau, D. J., and Con J. D., "Noise-reduction mechanism of a flat-plate serrated trailing-edge". *AIAA journal*, Vol. 51, No. 10, pp. 2513– 2522, 2013.

9 Soderman, P. T., "Leading-edge serrations which reduce the noise of low-speed rotors", NASA technical note, NASA TN D-7371, 1973.

10 Hersh, A. S., Soderman, P. T. and Hayden, R. E., "Investigation of acoustic effects of leading-edge serrations on airfoils", *AIAA journal*, Vol. 11, No. 4, pp. 197–202, 1974.

11 Lau, A. S. H., Haeri, S. and Kim, J. W., "The effect of wavy leading-edges on aerofoil-gust interaction noise", *Journal of Sound and Vibration*, Vol. 332, pp.6234–6253, 2013.

12 Clair, V., Polacsek, C., Le Garrec, T., Reboul, G., Gruber, M. and Joseph, P. F., "Experimental and numerical investigation of turbulence-airfoil noise reduction using wavy edges", *AIAA journal*, Vol. 51, No. 11, pp. 2695–2713, 2013.